CELL BIOLOGY

Mitochondrial metabolic regulation by GRP78

Manoj Prasad,[1] Kevin J. Pawlak,[1] William E. Burak,[1,2] Elizabeth E. Perry,[3] Brendan Marshall,[3] Randy M. Whittal,[4] Himangshu S. Bose[1,2]*

Steroids, essential for mammalian survival, are initiated by cholesterol transport by steroidogenic acute regulatory protein (StAR). Appropriate protein folding is an essential requirement of activity. Endoplasmic reticulum (ER) chaperones assist in folding of cytoplasmic proteins, whereas mitochondrial chaperones fold only mitochondrial proteins. We show that glucose regulatory protein 78 (GRP78), a master ER chaperone, is also present at the mitochondria-associated ER membrane (MAM), where it folds StAR for delivery to the outer mitochondrial membrane. StAR expression and activity are drastically reduced following GRP78 knockdown. StAR folding starts at the MAM region; thus, its cholesterol fostering capacity is regulated by GRP78 long before StAR reaches the mitochondria. In summary, GRP78 is an acute regulator of steroidogenesis at the MAM, regulating the intermediate folding of StAR that is crucial for its activity.

INTRODUCTION

Close direct or indirect connections between organelles are required for biological function. Even in moving organelles, such as mitochondria, physical connections with the endoplasmic reticulum (ER) have been observed (*1*) as electron-dense structures that bridge the organelles (*2*). Although mammalian ERMES (ER-mitochondria encounter structure) (*3*) expression had not been detected, a specialized subdomain, the mitochondria-associated ER membranes (MAM), physically connects the ER to mitochondria and provides a mitochondrial-ER axis that compartmentalizes both stress and metabolic signaling (*4*, *5*). The MAM, comprising a small section of the outer mitochondrial membrane (OMM) with the ER (*2*), defines a laterally differentiated subcompartment of the ER that is dedicated to performing lipid biosynthesis and perhaps other functions necessary for the mitochondrial membranes.

The successful intracellular routing of many proteins is also governed by a quality control system that recognizes particular structural motifs, retaining and degrading defective molecules given that abnormal proteins interfere with normal cellular function and eventually may result in cell death. Accumulation of aberrant conformations is limited by a chaperone system to assist the overall folding process (*6*–*8*). Chaperones increase the efficiency of the overall folding process by reducing the probability of aggregation, protecting proteins as they fold, and rescuing misfolded and aggregated proteins (*9*, *10*). The most abundant ER chaperone is the 78-kDa glucose-regulated protein (GRP78/BiP), which is responsible for maintaining the ER permeability barrier during protein translocation, guiding protein folding and assembly, and targeting misfolded proteins for degradation (*11*).

Steroid synthesis starts at the mitochondria. In an acute response or upon hormonal stimulation, steroidogenic acute regulatory protein (StAR) (*12*) is synthesized in the cytoplasm and then targeted to mitochondria to transport cholesterol from the OMM to the inner mitochondrial membrane (IMM). In the absence of StAR, no steroid is synthesized, resulting in death shortly after birth due to salt-losing crisis (*13*). After the StAR is loaded onto the OMM, it first interacts with the OMM-associated voltage-dependent anion channel 1 (VDAC1) (*14*, *15*) and then with VDAC2 (*16*) to obtain its active conformation, which is required for its translocation to the mitochondrial matrix as its final destination. However, its processing mechanism before mitochondrial import is unknown. Mutant and wild-type (WT) StAR interact with the VDACs and are processed into the mitochondria in a similar fashion (*16*), suggesting that StAR might go through multiple intermediate folding steps in the cytoplasm before it reaches the VDACs. Here, we show that GRP78 facilitates StAR intermediate state folding through a limited, transient interaction before its adoption of an active conformational state at the mitochondrial membrane that is suitable for cholesterol fostering and import. Mutant and WT StAR are folded differently by GRP78, but simultaneously, both are folded at the MAM. The transient state of folding governs the folding state required for its delivery onto the mitochondrial membrane. In the absence of the chaperone, intermediate folding is lost, and the unfolded protein is degraded (*9*, *10*), resulting in the ablation of StAR expression and complete shutdown of mitochondrial steroidogenesis. Thus, GRP78 is a critical regulator of mammalian survival by facilitating the intermediate folding of steroidogenic proteins, such as StAR, before their mitochondrial delivery, which is essential for mitochondrial function in adrenal and gonadal tissues.

RESULTS

Because cholesterol cannot be directly transported into mitochondria and requires lipid membranes as a carrier, a connection between the ER and mitochondria is necessary and/or the distance between the two organelles must be very close to permit its transport by a carrier protein. Because testicular cells are one of the highest steroid-producing cells in the mammalian system, we examined the mitochondria and ER in these cells by electron microscopy (EM). As shown in fig. S1 (A and B), mitochondria were in close proximity to the rough ER in testicular cells. The close distance between the organelles may be mediated through an interaction between the ER and mitochondrial proteins without involving covalent linkage. Thus, ER-resident proteins may facilitate the folding of transient MAM proteins, such as StAR, given the short distance between both organelles (*2*).

To identify the proteins that may be involved in the interaction between these two organelles, we isolated ER, MAM, and mitochondrial fractions from rat testes. We observed a 450-kDa native StAR-containing complex from the digitonin lysate of the MAM fraction (Fig. 1A, left) (*16*). Upon hormonal stimulation, the newly synthesized

[1]Laboratory of Biochemistry and Cell Biology, Department of Biomedical Sciences, Mercer University School of Medicine, Savannah, GA 31404, USA. [2]Anderson Cancer Institute, Memorial University Medical Center, Savannah, GA 31404, USA. [3]Department of Cellular Biology and Anatomy, Augusta University, Augusta, GA 30912, USA. [4]Department of Chemistry, University of Alberta, Edmonton, Alberta T6G 2G2, Canada. *Corresponding author. Email: bose_hs@mercer.edu

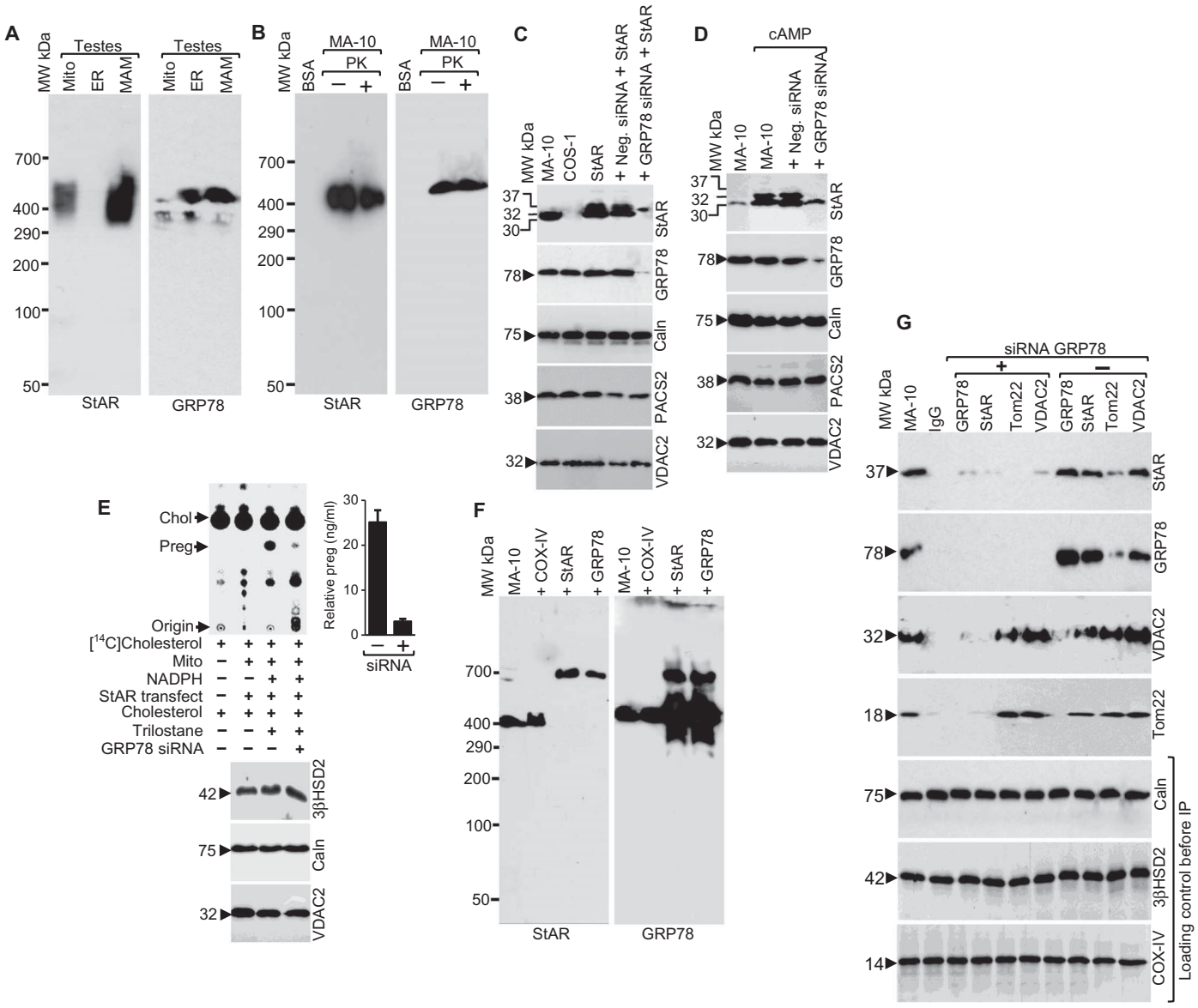

Fig. 1. ER and mitochondria are located in close proximity in murine testis. (**A**) Identification of 450-kDa StAR- and GRP78-containing complex in the testis through native gradient PAGE after solubilization with digitonin and staining the different organelle fractions with StAR and GRP78 antibodies independently. MW, molecular weight. (**B**) Identification of the 450-kDa complex after solubilizing cAMP-stimulated mouse Leydig MA-10 cells with digitonin, electrophoresis through native gradient PAGE, and staining with StAR (left) and GRP78 (right) antibodies in the absence and presence of PK (0.25 μg/μl) for 30 min. (**C** and **D**) Role of GRP78 in StAR expression. (C) COS-1 cells expressing StAR were transfected with GRP78 siRNA, and GRP78 expression was determined by Western blot analysis. In the absence of GRP78, StAR expression was almost absent, but not with the negative control siRNA. (D) MA-10 cells were stimulated with cAMP, and experiments were performed as in (C). The bottom panels confirm that the expression of Caln, PACS2, and VDAC2 remained unchanged in both COS-1 (C) and MA-10 (D) cells. (**E**) (Left) Measurement of pregnenolone synthesis after knockdown of steroidogenic MA-10 cells with GRP78 siRNA. (Bottom) 3βHSD2 and Caln levels, confirming that equal amounts of protein were applied in each reaction. (Right) Quantitative measurement of pregnenolone synthesized. Data in (E) are means ± SEM of three independent siRNA experiments performed at three different times. (**F**) Antibody shift experiment after incubation of the indicated antibodies of the MAM fraction isolated from rat testes followed by analysis through a native gradient PAGE and staining with GRP78 and StAR antibodies independently. (**G**) Coimmunoprecipitation with the indicated antibodies followed by Western blotting with StAR, GRP78, VDAC2, and Tom22 antibodies independently in the absence and presence of GRP78 siRNA. The bottom panel shows the staining with Caln, 3βHSD2, and COX-IV antibodies before the immunoprecipitation (IP) experiment.

StAR is present as a 37-kDa precursor protein at the MAM. Next, the precursor forms an intermediate 32-kDa protein before its mitochondrial entry, eventually maturing to a 30-kDa protein after its import into the mitochondria (*16*). Mass spectrometric (MS) examination of the MAM fraction also showed the presence of GRP78 in the complex 50% of the time (table S1). GRP78 is a master chaperone for both cytoplasmic and membrane-associated proteins. Thus, we hypothesized that it is the ultimate regulator to initiate metabolic activity through StAR folding at the MAM, which is required for its subsequent targeting to the OMM. Native gradient polyacrylamide gel electrophoresis

(PAGE) showed a similar 450-kDa complex containing GRP78 in the ER and MAM fractions (Fig. 1A, right). MS analysis of the MAM fraction identified similar proteins as seen for StAR (table S2). A similar 450-kDa complex was present in MA-10 cells even when incubated in the presence of proteinase K (PK) (0.25 μg/μl) for 30 min (Fig. 1B), suggesting a strong interaction between StAR- and GRP78-associated proteins.

EM (fig. S1, C to H) and biochemical fractionation (fig. S2) experiments show the localization of StAR and GRP78 in the ER, MAM, and mitochondria. Because GRP78 is a highly abundant chaperone at the ER that interacts with StAR, it is likely facilitating its folding and subsequent activity (*17*). We next knocked down the expression of GRP78 by small interfering RNA (siRNA) in COS-1 cells (Fig. 1C) or adenosine 3′,5′-monophosphate (cAMP)–stimulated MA-10 cells (Fig. 1D) and identified changes in StAR expression by Western blotting. In the absence of GRP78, the expression of StAR was greatly reduced, but the negative control siRNA had no effect, suggesting that GRP78 is responsible for StAR expression. As expected, the absence of GRP78 did not affect the expression of mitochondrial VDAC2 or the ER proteins PACS2 and calnexin (Caln) (Fig. 1, C and D). As shown in Fig. 1E, pregnenolone synthesis in MA-10 cells decreased from 25 ng/ml in control cells to 2 ng/ml in the absence of GRP78. The expression of OMM-associated VDAC2 or ER-associated Caln was unchanged (Fig. 1E, bottom). The expression of 3β-hydroxysteroid dehydrogenase 2 (3βHSD2) (Fig. 1E, bottom panel), which catalyzes pregnenolone to progesterone conversion, was not affected, confirming that the mitochondrial enzymatic capacity was not affected beyond altered StAR expression and, therefore, cholesterol fostering.

Because GRP78 is a predominantly MAM-associated protein toward the ER side, the interaction between the GRP78 and StAR is likely early after StAR synthesis at the ER. To confirm association of GRP78 in the StAR-containing complex, we performed antibody shift experiments with StAR and GRP78 antibodies independently of digitonin lysates isolated from cAMP-stimulated MA-10 cells following native gradient PAGE. As shown in Fig. 1F, both StAR- and GRP78-containing complexes were supershifted with StAR and GRP78 antibodies, as evidenced by Western blotting with StAR (Fig. 1F, left) and GRP78 (Fig. 1F, right) antibodies independently. GRP78 is a highly abundant chaperonic protein, unlike StAR, which is expressed on cAMP stimulation. A significant excess of StAR-unbound GRP78 remains in the MAM region, which can be identified by a 400-kDa unbound complex when stained with GRP78 antibody. In addition, when staining with the StAR antibody, limited expression was observed and a similar unbound 400-kDa complex was not observed. This follows with our observations because the quantity of StAR protein is thought to be the limiting factor with the abundantly available GRP78. In summary, these results confirm that the master chaperone GRP78 possibly plays a role in StAR expression and activity.

To confirm that GRP78 and StAR directly interact, we performed coimmunoprecipitation experiments in the absence or presence of GRP78 knockdown in MA-10 cells stimulated with cAMP. In the absence of GRP78 knockdown, the GRP78 antibody pulled out StAR, and the StAR antibody pulled out GRP78 (Fig. 1G). As expected, no interaction with GRP78, Tom22, or VDAC2 was observed after knocking down GRP78 (Fig. 1G). The expression of Caln, 3βHSD2, and cytochrome c oxidase IV (COX-IV) was analyzed to confirm that the total amount of protein was similar in coimmunoprecipitation experiments (Fig. 1G, bottom).

Upon physiological demand or hormonal stimulation, adrenal and gonadal cells synthesize StAR (*18*, *19*) as an immediate need for mitochondrial cholesterol fostering, where complete folding is likely the last step (*17*) in which the protein is inactive (*12*). Thus, we hypothesized that GRP78 is responsible for maintaining StAR in an active, intermediate state so that it can be delivered to the OMM and that the proteins interact transiently on the order of magnitude of minutes rather than seconds. Thus, we studied the kinetics of formation of a 750-kDa complex by supershifting with GRP78 and StAR antibodies in lysates from MA-10 cells stimulated with cAMP (Fig. 2, A and B). In the absence of cAMP, only the 450-kDa GRP78-containing complex was detected; however, after 30 min, a high–molecular weight 750-kDa complex was formed that was maintained for 6 hours, at which point only the 450-kDa complex was observed (Fig. 2A, top panel). Identical results were obtained using a StAR antibody (Fig. 2B, top panel), confirming that StAR remains associated with GRP78 for about 6 hours, with maximum interaction in approximately 3 hours. It is possible that at 3 hours, GRP78 is saturated; therefore, newly synthesized proteins can not be folded until folded StAR is released from the GRP78 core. At 6 hours, it is possible that all the MAM-associated proteins are imported into the mitochondria, resulting in the reduction of the upper complex.

We hypothesized that StAR and GRP78 may interact at the MAM immediately upon cAMP stimulation in a manner that coincides with GRP78 localization at the MAM. After stimulation of MA-10 cells with cAMP for 30 min to 24 hours, we determined the distribution pattern of StAR and GRP78 in ER, MAM, and mitochondrial fractions by Western blot analysis. As shown in Fig. 2C, StAR translocated from the ER to the MAM and mitochondria at 3 hours following cAMP stimulation. The intensity of StAR expression at the MAM remained the same from 3 to 24 hours; however, the intensity at the mitochondrial membrane increased (Fig. 2C). Because of its mitochondrial targeting, the residency time of StAR at the ER and MAM was short. Because StAR import into the mitochondria is slower than observed for other mitochondrial targeted proteins (*17*), a bulk of the unimported StAR remains at the OMM. Semiquantitative estimations of the band intensities are shown in Fig. 2D, which shows StAR translocation from the ER by 3 hours following cAMP stimulation, whereas the residency time at the MAM remains unchanged over time. The amount of protein present at the MAM is more than at the ER at any given time, suggesting a short residency time in this organelle (Fig. 2D). We have summarized these observations in the form of a cartoon, showing the association of the StAR precursor protein with GRP78, forming a 750-kDa complex and a 450-kDa complex for a short time with cAMP stimulation (Fig. 2E). Once all the precursor protein is released, a new round of precursor is associated with GRP78 for the next step of folding. Once the precursor is released from the GRP78 core, it comes close to the mitochondria, forming a 32-kDa intermediate form and release from the 750-kDa complex. In the next step, all the precursor protein is imported and StAR is a 30-kDa mitochondrial-associated protein, resulting in only one 450-kDa complex.

To validate compartment-specific expression observed through immuno-EM (fig. S3), we stimulated MA-10 cells with cAMP in a similar fashion to EM localization and stained ER, MAM, and mitochondrial fractions with StAR and GRP78 antibodies. The Western blotting results of StAR (Fig. 3, A and B) and GRP78 (Fig. 3, C and D) are similar to the EM experiments. StAR expression increased at the MAM after 1 hour and then decreased with higher expression at the

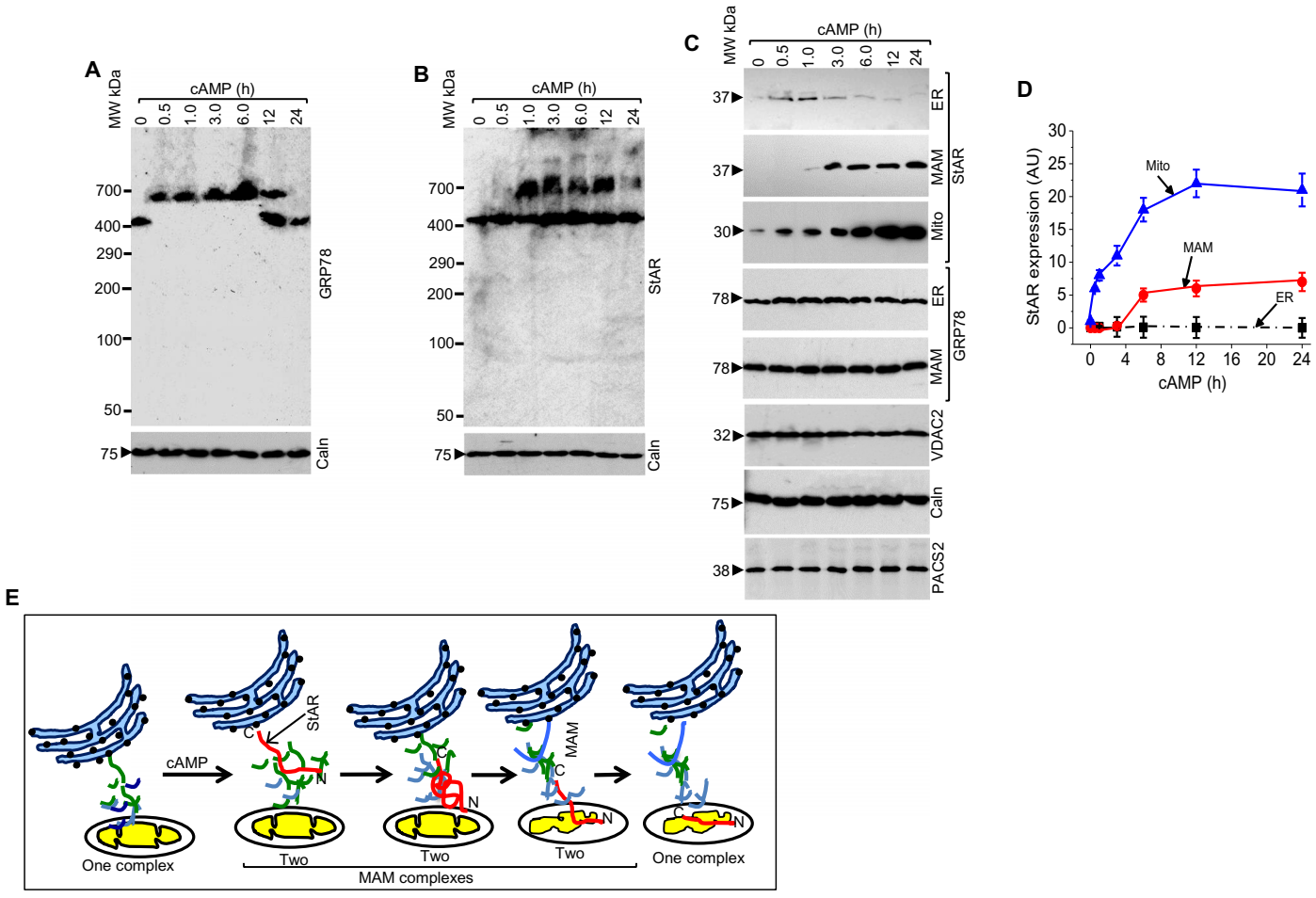

Fig. 2. GRP78 and StAR are closely associated for a limited time. (**A** and **B**) Kinetics of the antibody shift in cAMP-stimulated MA-10 cells treated for the indicated times and analyzed in native gradient PAGE, where they were first incubated with StAR (A) and GRP78 (B) antibodies independently followed by staining with GRP78 (A) and StAR (B) antibodies, showing that the interaction between GRP78 and StAR started after 30 min. Caln staining showed an equivalent amount of protein present in each reaction. (**C**) Kinetics of StAR overexpression in MA-10 cells after cAMP stimulation with the indicated times in the ER, MAM, and mitochondrial fractions. The ER and MAM fractions were also stained with GRP78 antibody. The bottom panels show unchanged expression of PACS2, VDAC2, and Caln on cAMP stimulation, as evidenced by staining with the indicated antibodies. (**D**) Quantitative analysis of StAR expression in ER, MAM, and mitochondrial fractions after stimulation with cAMP. StAR remained at a similar level in the MAM and ER, but it continuously increased with time in the mitochondria. GRP78 expression in the MAM remained unchanged over time with cAMP stimulation. Data are means ± SEM of independent experiments performed at least three times. AU, arbitrary units. (**E**) Schematic presentation of the antibody shift analyses, where GRP78 forms a 450-kDa complex with the associated proteins but, upon stimulation with cAMP after 30 min, forms a high–molecular weight 750-kDa complex, because of the increased synthesis of StAR precursor, and continues to form a complex over 6 hours, resulting in two complexes. After 6 hours, precursor StAR is imported into the mitochondria, resulting in one complex again.

mitochondria after 6 hours. Immuno-EM localization of StAR around MAM or OMM shows a better expression at 30 min as compared to the Western blot staining with StAR antibody (Fig. 3B). As cAMP stimulation continues, StAR levels increase gradually, passing through the GRP78 chaperonic core and resulting in a more folded form required for delivery to the OMM (Fig. 3E). The colocalization of StAR and GRP78 at the MAM was shown with EM analysis of MA-10 cells after stimulation with cAMP by probing the cells with GRP78 and StAR antibodies together (fig. S5). In summary, we conclude that the master chaperone GRP78 may facilitate StAR folding during its transient passage through the MAM before loading onto the OMM.

The above result suggests that StAR is in a dynamic condition with gradual changes in folding mediated by GRP78. To confirm that GRP78 and StAR were transiently localized, we performed density gradient centrifugation after stimulation of MA-10 cells with cAMP over various time points. As shown in Fig. 4A and fig. S6, StAR and GRP78 were identified in the same fractions (fractions 5 to 9) after 1 hour of stimulation with cAMP. At 4 hours following cAMP stimulation, StAR was identified in lanes 8 to 14; GRP78 also moved to fractions 9 to 15, suggesting that StAR moved minimally as compared to GRP78 (Fig. 4A and fig. S6), which is likely due to a loose association with GRP78 and release from the GRP78 core to the mitochondrial membrane. We have presented the scenario in the form of a cartoon, where GRP78 is available for interaction with StAR after its expression, remaining for almost 3 hours until StAR moves further toward the OMM (Fig. 4B).

Because GRP78 functions at the MAM, we hypothesized that StAR folding starts at the MAM and is different for mutant proteins. To evaluate this hypothesis, we selected a mutant StAR, R182L, which was identified as a founder mutation in Arab patients (*17*, *18*), overexpressed

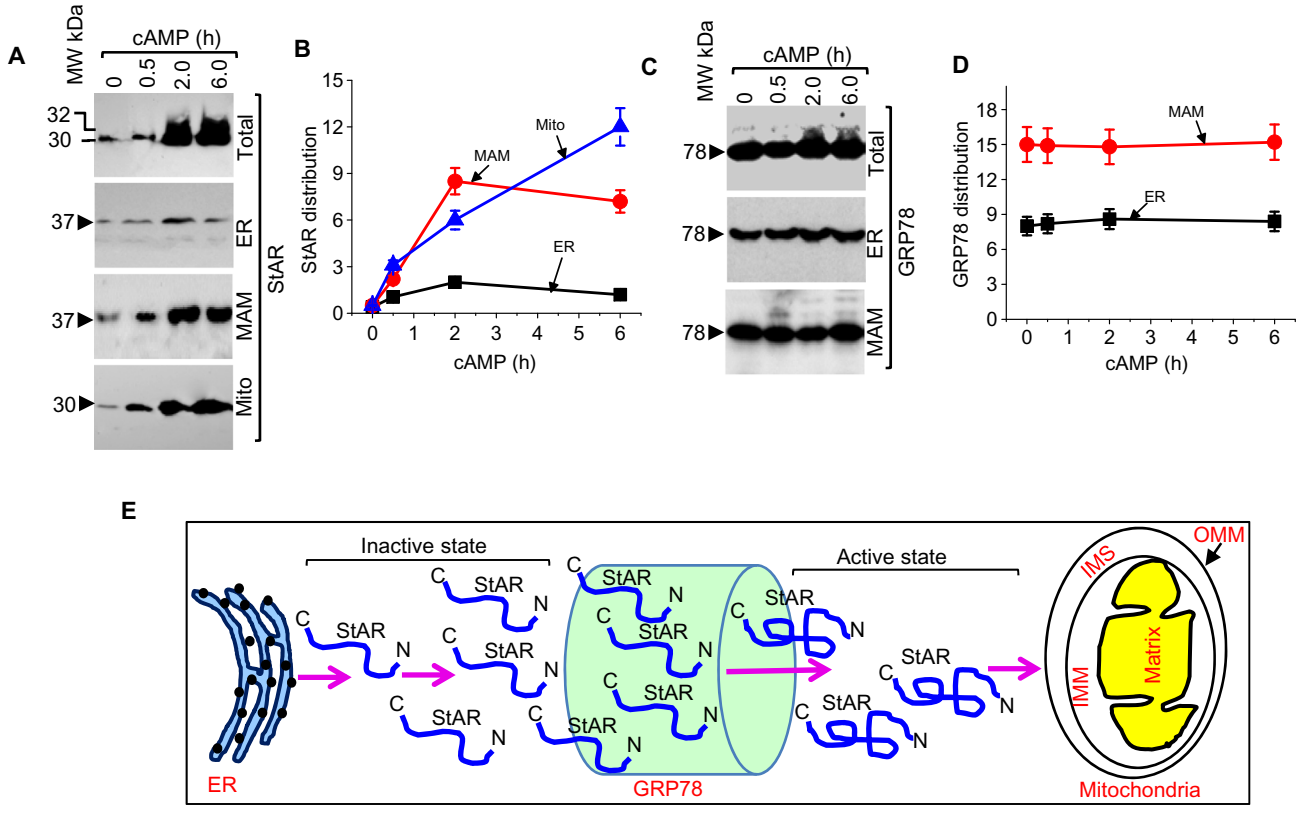

Fig. 3. Kinetics of StAR folding by GRP78. (**A**) Expression of StAR at the ER, MAM, and mitochondrial compartment after cAMP stimulation for 30 min, 2 hours, and 6 hours. The MAM and ER fractions were isolated by Percoll density gradient. (**B**) Quantitative estimation of the density distribution identified in (A). (**C**) Expression of GRP78 at the ER, MAM, and total lysate after cAMP stimulation for 30 min, 2 hours, and 6 hours. (**D**) Quantitative estimation of the density distribution identified in (C). (**E**) Cartoon describing the mechanism of StAR progression through the GRP78 chaperone. StAR is released immediately in the steroidogenic tissue upon stress or hormonal stimulation, and the amount of expression increased gradually. After passing through the GRP78 chaperone core, the folded StAR arrives at the OMM for its next function. IMM, inner mitochondrial membrane; IMS, inter membranous space.

it in COS-1 cells, isolated the MAM fraction, and analyzed its folding by limited proteolysis with PK compared to WT StAR (Fig. 4C). As shown in Fig. 4D (left panel), WT StAR was gradually proteolyzed with increasing concentrations of PK; 70% was proteolyzed with PK (0.2 μg/μl). In contrast, R182L StAR was almost completely proteolyzed at PK (0.1 μg/μl), suggesting that its folding was different from the WT at the MAM. A quantitative analysis of the resistance of proteolysis pattern between WT and R182L confirms our claim (Fig. 4D, right panel). In contrast, the proteolysis pattern of GRP78 was identical, and the total protein content was identical when it was stained with StAR and GRP78 antibodies independently before proteolysis (Fig. 4D, bottom panels). Overexpression of WT or R182L StAR in COS-1 cells shows complete absence of StAR and GRP78 in the GRP78 knockdown cells, but the expression of VDAC2 or Caln was unchanged (Fig. 4E). Density gradient fractionation of R182L StAR stained with StAR antibody showed that the GRP78 (fractions 3 to 11) remained associated longer with the WT (fractions 3 to 10) as compared to R182L StAR (fractions 2 to 6). In addition, cell-free synthesis (CFS) in rabbit reticulocyte system synthesizes the protein in a form similar to the native-like (*20*). We determined the difference in folding between the WT and R182L StAR by limited proteolysis with PK. The mutant protein was proteolyzed faster as compared to WT (Fig. 4G), suggesting that the mutant R182L StAR was less tightly folded than the WT. In summary, these results suggest that GRP78 folds WT and mutant StAR differently at the MAM.

StAR has domains that may bind lipids (*21*), suggesting a possibility of its presence within lipid rafts, which may facilitate cholesterol movement from the raft to the mitochondria. The raft is a part of MAM and it contains sphingomyelin (SM), which is a major sphingolipid, comprising approximately 10% phospholipid in mammalian cells. Together with cholesterol, SM forms specific liquid-ordered domains in membranes (*22*, *23*). By fluorescence resonance energy transfer, we observed that the binding of StAR with phospholipids was increased in the presence of cholesterol (*15*, *24*). Protein finger printing experiments indicated an interaction of the StAR C terminus with lipid vesicles (*25*). However, such an interaction would likely be transient and promote the immediate folding of StAR before it reaches the mitochondria. To confirm this hypothesis, we first isolated rafts from cAMP-stimulated MA-10 cells and immunoblotted them with a StAR antibody. As shown in Fig. 5A, cAMP-stimulated cell lysates showed two bands, the 37-kDa precursor and the 32-kDa intermediate StAR. However, the purified raft had only the 37-kDa precursor band (Fig. 5A). StAR is active in an unfolded conformation (*26*). It is likely that the 37-kDa StAR is the partially unfolded conformation that interacts with the phospholipids present in the raft. Having a mitochondrial targeting sequence at the N terminus, StAR leaves the raft quickly and localizes at the mitochondrial matrix as a final destination (*12*). So, we can intuitively consider that the protein is processed from the raft to the mitochondria.

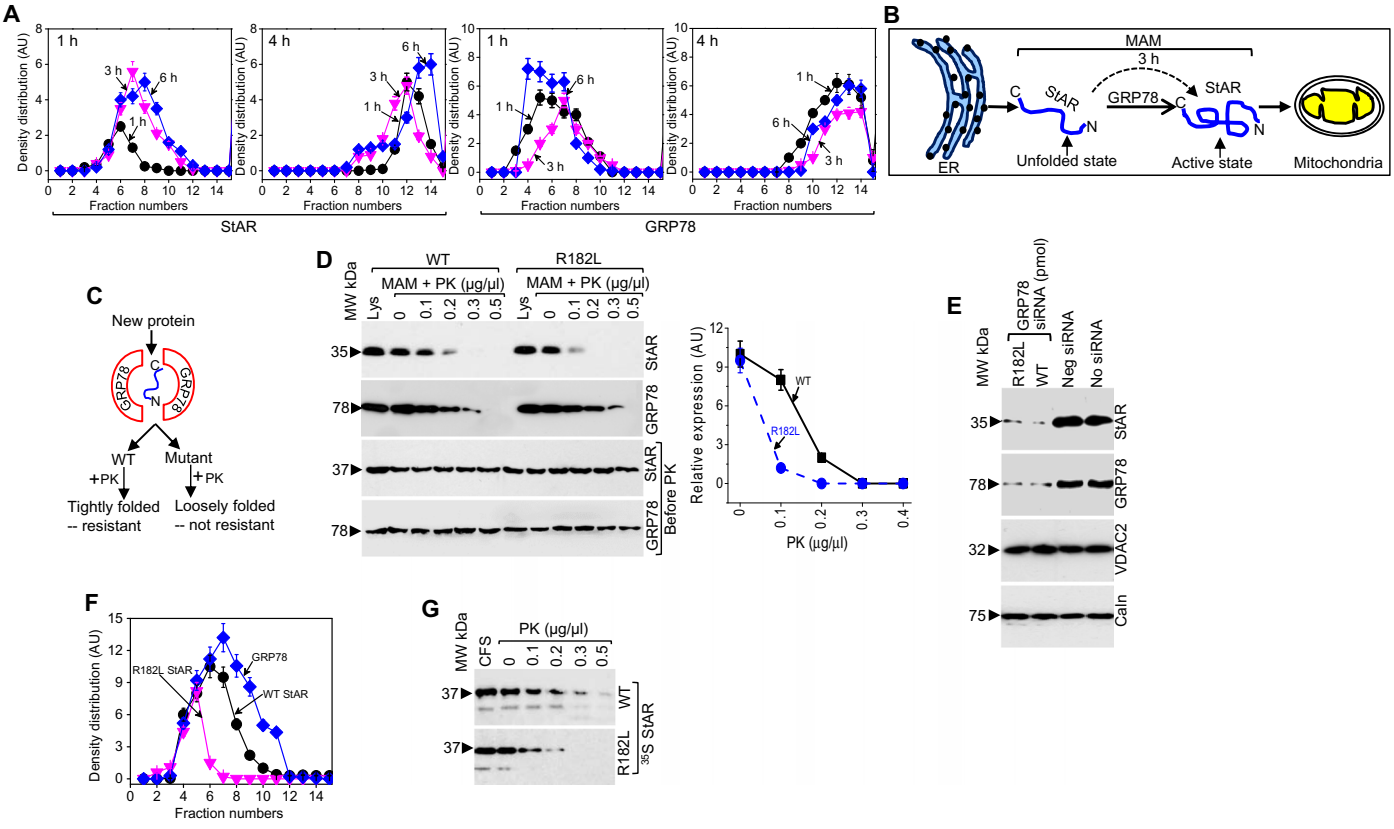

Fig. 4. Colocalization kinetics of StAR and GRP78 after cAMP stimulation. (**A**) Quantitative analysis of sucrose density gradient fractionation of MA-10 cells stimulated with cAMP for the indicated times. The density fractions were analyzed by SDS-PAGE and staining with StAR and GRP78 antibodies independently after 1 and 4 hours of centrifugation. Data are means ± SEM of at least three different experiments performed at three different times. (**B**) The cartoon shows that GRP78 is loosely associated with StAR and quickly moves to the lower fraction, whereas it takes more than 3 hours for StAR to transition from an open, unfolded conformation to a more folded conformation, which is possibly an active conformation. (**C**) Cartoon showing that the identical folding step is followed for both the mutant and WT StAR. Because the two proteins are folded differently, one (WT) is more resistant to proteolysis than the other (mutant). (**D**) (Left) Proteolysis of purified MAM fractions after overexpression of WT and mutant (R182L) StAR with indicated concentrations of PK. The bottom panels (before PK) show staining with StAR and GRP78 before proteolysis, confirming equal levels of protein. (Right) Quantitative analysis of the degree of protection from proteolysis in the left panel. (**E**) COS-1 cells expressing WT and mutant (R182L) StAR were transfected with GRP78 siRNA. GRP78 and StAR expression was determined by Western blot analysis. Mutant and WT StAR expression was almost absent with GRP78 siRNA, but not with the negative control siRNA. The bottom panels confirm that the expression of VDAC2 and Caln remained unchanged. (**F**) Quantitative analysis of sucrose density gradient fractionation of COS-1 cells overexpressing WT and mutant R182L StAR. The density fractions were analyzed by SDS-PAGE and staining with StAR and GRP78 antibodies independently after 1 hour of centrifugation. (**G**) Limited proteolysis of the [^{35}S]methionine-labeled cell-free synthesized (CFS) WT and mutant StAR with indicated concentrations of PK for 30 min at 4°C.

To understand how long StAR remains at the raft before transiting to the MAM, we isolated rafts and MAM from MA-10 cells after varying time points following cAMP stimulation. Although GRP78 expression was not altered in the whole-cell lysates (Fig. 5B, middle panels), MAM fraction (Fig. 5C, middle panels), or raft fraction (Fig. 5D, middle panels), StAR expression was induced in the total cell lysate at 3 hours following cAMP stimulation (Fig. 5B, top panel). Analysis of the MAM fractions showed that StAR expression also started at 3 hours (Fig. 5C, top panel); however, its expression in rafts was observed at 1 hour (Fig. 5D, top panel), suggesting that the StAR moves from the raft to the MAM and that GRP78 may facilitate folding at both the raft and MAM. Analysis of Caln expression confirmed that the same amount of total protein was applied in each experimental lane (Fig. 5, B to D, bottom panels). Quantitative analysis showed that StAR expression increased continuously from 3 to 12 hours in the whole-cell lysates, which contain MAM and mitochondria, after which it remained unchanged (Fig. 5E). In contrast, the expression pattern in the MAM was very high at 3 hours and reached a plateau at 6 hours (Fig. 5E), suggesting that StAR is moving from the rafts to the MAM. In the rafts, StAR levels continuously increased until 7.5 hours, possibly due to its movement to the MAM (Fig. 5E).

To understand whether StAR and GRP78 interact with each other during their residency at the MAM and to evaluate their proximity, we performed in vitro chemical cross-linking immediately after isolation of the MAM. As shown in Fig. 5F, staining MAM fractions with a StAR antibody resulted in a prominent 115-kDa band with 1 mM BS3, increasing to maximal intensity with 2 mM BS3 and then decreasing with 5 mM. However, the same cross-linked complex was not observed in the mitochondrial fractions. Uncross-linked 37-kDa StAR was also evident, as well as a small cross-linked band of 70 kDa, which may be due to an interaction between VDAC and StAR (*16*). MS analysis of the 70-kDa band showed the presence of StAR and VDAC2, and the 115-kDa band showed the presence of GRP78, StAR, and VDAC2 (table S3). A parallel experiment analyzing GRP78

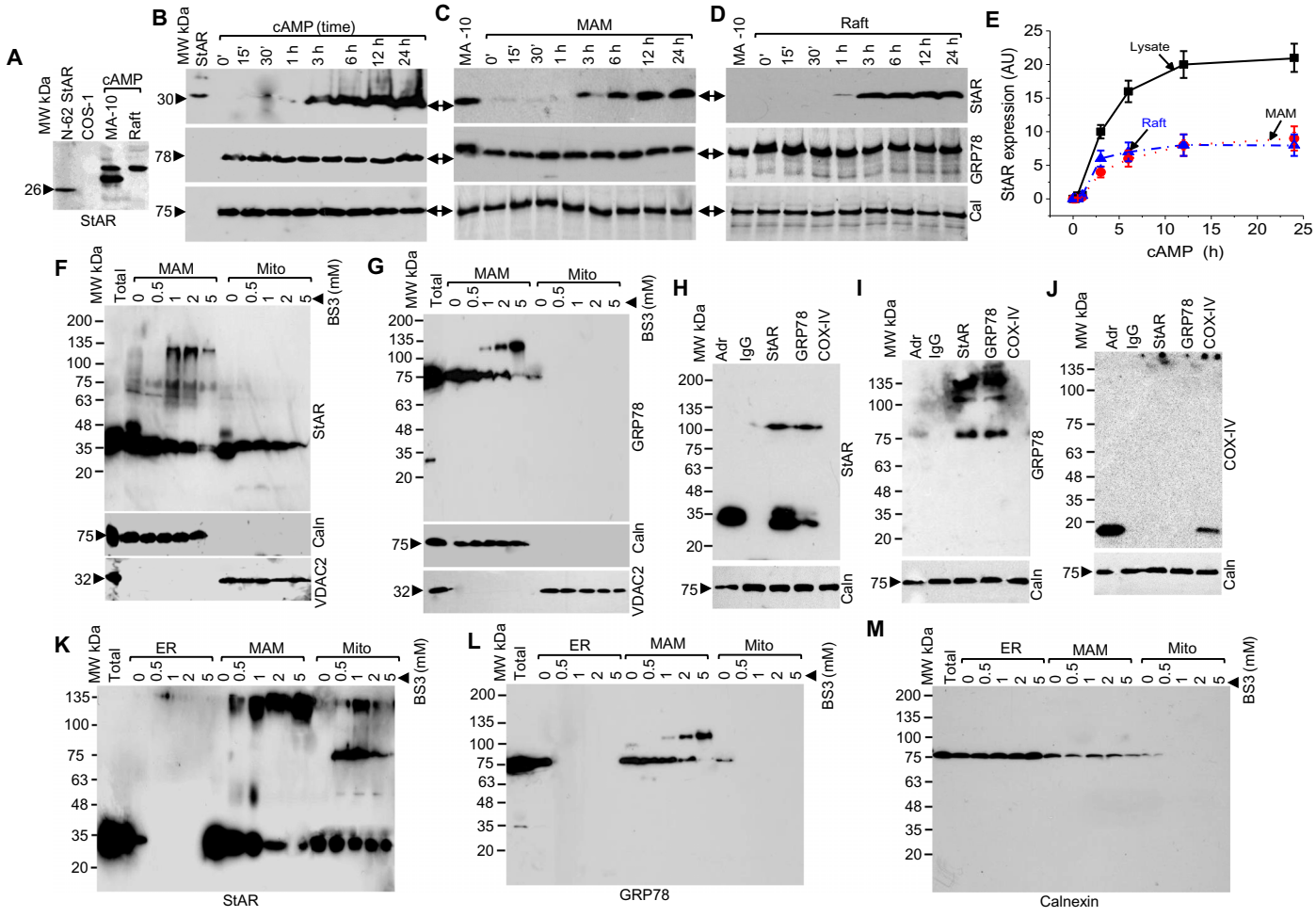

Fig. 5. Mechanism of StAR transport from lipid rafts to the MAM. (**A**) Isolation of rafts from cAMP-stimulated MA-10 cells stained with StAR antibody. (**B** to **D**) Determination of StAR levels in the whole-cell lysate (B), MAM (C), and raft (D) fractions after stimulation of the MA-10 cells with cAMP for the indicated times. The amount of StAR remained the same in the raft but gradually increased in the MAM. The middle panels show the expression of GRP78, which remained unchanged with cAMP stimulation. (**E**) Quantitative analysis of StAR distribution in the MAM and raft fractions, showing that StAR is localized to the raft earlier than MAM. (**F** and **G**) Chemical cross-linking with varying concentrations of the cross-linker BS3, added to purified MAM and mitochondria isolated from cAMP-stimulated MA-10 cells and stained with StAR (F) and GRP78 (G) antibodies independently. The bottom panels show the equal amount of protein for each cross-linking reaction before the start of the cross-linking by staining with Caln and VDAC2 antibodies. (**H** to **J**) Coimmunoprecipitation of the cross-linking reaction (2 mM BS3) of the MAM fractions isolated from the cAMP-stimulated MA-10 cells with GRP78, StAR, and COX-IV antibodies followed by Western blotting with StAR (H, top), GRP78 (I, top), and COX-IV (J, top) antibodies independently. The bottom panels show the same amount of MAM protein applied in each experiment when stained with Caln antibody. (**K** to **M**) In vivo chemical cross-linking of cAMP-stimulated MA-10 cells followed by purification of the ER, MAM, and mitochondria stained with StAR (K), GRP78 (L), and Caln (M) antibodies independently. Staining the same membrane with Caln confirmed that similar amounts of protein were present in each reaction. Data in (E) are means ± SEM of at least three different experiments performed at three different times.

confirmed the presence of the 78-kDa uncross-linked protein and a 115-kDa band with 1 mM cross-linker at the MAM and not in the mitochondria (Fig. 5G). In addition, the 78-kDa GRP78 band decreased with increasing intensity of the 115-kDa band, completely disappearing with 5 mM BS3, confirming that the interaction between GRP78 and StAR was direct. Coimmunoprecipitation of the cross-linked reaction and staining with GRP78 and StAR antibodies pulled out the major complex (Fig. 5, H and I, top panels); however, it was not detected by immunoprecipitation with the mitochondrial marker COX-IV (Fig. 5J, top panel), confirming that StAR and GRP78 interact in the MAM.

Although purified MAM fractions cross-linked GRP78 and StAR well, we wanted to determine whether these proteins interact in vivo. Thus, we stimulated MA-10 cells with cAMP, performed in vivo chemical cross-linking of whole cells with various concentrations of BS3, and isolated the ER and MAM fractions by Percoll density gradient centrifugation and analyzed them by Western blotting with StAR (Fig. 5K), GRP78 (Fig. 5L), and Caln (Fig. 5M) antibodies independently. As shown in Fig. 5L, a high–molecular weight band of 115 kDa was first observed in the MAM fractions. There was no cross-linking with the ER or mitochondrial fractions because StAR is absent in the ER and GRP78 is absent in the mitochondria. Staining the membrane with a Caln antibody confirmed that the same amount of protein was present in the ER and MAM fractions (Fig. 5M). Because Caln is an ER marker, most was present in the ER, with a minor amount in the mitochondria. In summary, these results confirm that GRP78 and StAR interact in the cell long before StAR reaches the OMM; thus, docking of StAR starts at the raft.

DISCUSSION

The MAM is the central hub for all mitochondrial metabolic regulation, where StAR transits following its synthesis on acute regulation before it reaches its final destination, the mitochondria. Thus, the mitochondrial metabolic regulation is mediated by a MAM protein. EM analysis of the ER and mitochondria in the testes revealed that the distance between the two organelles is extremely short, which may facilitate rapid steroidogenesis on demand that may be specific for testis. As a protein, StAR cannot directly interact with cholesterol; therefore, this interaction may be mediated through raft. The adrenal and gonads are already loaded with cholesterol at the OMM; therefore, StAR may foster it to the mitochondria while at the MAM, suggesting that its OMM localization is not a requirement for activity. This observation also explains why StAR is active without the N-terminal targeting sequence or why StARD3 has half the activity of StAR, whereas StARD4 has about 30% activity (*17*).

Because GRP78 is present in the MAM and total cell lysate at similar levels, it is likely that it facilitates StAR folding immediately after its release during acute hormonal demand or stress. The raft fractions also contained a minimal amount of GRP78, suggesting that it likely acts predominantly at the MAM rather than at the raft. Thus, GRP78 likely facilitates the folding of lipid-binding domain, which is also the region responsible for cholesterol fostering into the mitochondria. As a result, the N-signal sequence may remain unfolded to mediate mitochondrial import once the lipid-binding domain is at the MAM region. However, the import mechanism of StAR remains unchanged as long as the N-terminal sequence is unaltered. In conclusion, we show that GRP78 is necessary for StAR expression and activity by facilitating its appropriate folding. In the absence of GRP78, the protein is not folded and thus is likely proteolyzed because of its mislocalization. Thus, GRP78 is the first crucial regulator of steroidogenesis.

MATERIALS AND METHODS

Animals and compartmental fractionation of ER, MAM, and mitochondria

Animals.

Male Sprague-Dawley rats, 12 weeks of age, were purchased from Harlan/Sprague Dawley and fed Purina chow (Harlan Teklad Global Diets) and water. The animal procedure was approved by the institutional review board [Institutional Animal Care and Use Committee (IACUC) no. A1406011] on 8 September 2014. The animals were housed and mechanically ventilated with oxygen-enriched room air using a rodent respirator (Harvard Rodent Ventilator Model 683); the rate was adjusted to 30 to 40 breaths per minute, and tidal volume was set to 1.1 to 1.3 ml/100 g of body weight. Procedures for the isolation of adrenals and gonads were performed under sterile conditions. The body temperature was maintained at 37°C by a heating pad. IACUC guidelines were followed with animal subjects.

Compartmental fractionation of ER, MAM, and mitochondria.

To isolate the MAM from testis, four testes were pooled from the same group of animals, and the tissues were transferred to the mitochondrial isolation buffer [250 mM sucrose, 10 mM Hepes, and 1 mM EGTA (pH 7.4)] and diced into small pieces on ice. Tissue fractions were homogenized in a handheld all-glass Dounce homogenizer with 10 gentle up and down strokes, and the cell debris was removed by centrifugation at 3500*g* for 10 min and then by a procedure similar to fractionation from cells. To isolate the MAM from MA-10 cells, about 10×10^6 cells were used for each experiment. In brief, steroidogenic MA-10 cells were washed twice with phosphate-buffered saline (PBS) at room temperature and collected by centrifugation at 600*g* for 10 min and then resuspended in 500 µl of 10 mM Hepes (pH 7.4) for 30 min. Next, the cells were diluted further with 800 µl of mitochondrial isolation buffer and homogenized using 45 strokes in an all-glass Dounce homogenizer. The large debris and nuclei were separated by centrifugation twice at 600*g* for 10 min. Further centrifugation of the supernatant for 10 min at 10,300*g* was performed to isolate the crude mitochondria from the pellet. For the isolation of ER, we centrifuged the supernatant at 100,000*g* for 1 hour. To isolate pure mitochondrial fractions (*27*), we resuspended the crude mitochondrial pellet in isolation medium [250 mM mannitol, 5 mM Hepes (pH 7.4), 0.5 mM EGTA, and 0.1% bovine serum albumin (BSA)] using a Dounce homogenizer to a final volume of 2.0 ml and layered the crude mitochondrial suspension on top of a medium containing the density gradient buffer [225 mM mannitol, 25 mM Hepes (pH 7.4), 1 mM EGTA, 0.1% BSA, and 30% Percoll (v/v)]. After centrifugation at 95,000*g* for 30 min, the mitochondrial fraction was isolated two-thirds of the way down the tube, and the MAM complex was found directly above the mitochondrial fraction. The mitochondrial fractions were isolated using a thin Pasteur pipette and washed to remove the Percoll by first diluting them with isolation medium followed by centrifugation twice at 6300*g* for 10 min. The final mitochondrial pellet was resuspended in isolation medium and stored at −86°C. For isolation of the MAM fraction, the complex was washed to remove the Percoll by centrifugation at 6300*g* for 10 min followed by further centrifugation of the supernatant at 100,000*g*. The resultant MAM fraction was resuspended in 0.5 ml of buffer containing 0.25 M sucrose, 10 mM tris-HCl (pH 7.4), and 0.1 mM phenylmethylsulfonyl fluoride (PMSF) and stored at −70°C.

Cell culture, transfection, and knockdown experiments

Cell culture, transfections, and mitochondrial isolation from cultured cells were performed following our previously described procedure (*14*, *28*, *29*). Briefly, MA-10 cells were grown in Waymouth medium containing 5% fetal calf serum and 10% horse serum supplemented with 1× gentamicin and L-glutamine. COS-1 cells were cultured in Dulbecco's modified Eagle's medium with high glucose supplemented with 10% fetal bovine serum and penicillin-streptomycin. For StAR transfection, COS-1 cells were plated at a density of 30,000 cells per well in a six-well plate 18 hours before transfection. The cells were first washed with PBS and then with serum-free medium 12 hours after transfections and supplemented with medium containing appropriate antibiotics (10% serum). For GRP78 siRNA knockdown experiments, 30 or 60 pmol of sense (5′-CAGCAACUGGUUAAAGAUUUCUUCA-3′) and antisense (5′-UGAAGAACUCUUUAACCAGUUGCUG-3′) was used for transfection mixed with Oligofectamine (Life Technologies), used as a carrier, and processed for Western blotting or activity determination as described before with no modification (*14*, *28*, *29*). In some cases, trilostane (100 ng/ml) (a gift from G. Vinson, University of London) was added as an inhibitor of 3βHSD2.

Isolation of lipid rafts

The rafts were isolated from MA-10 cells following a protocol with modifications (*30*, *31*). When the MA-10 cells reached 80% confluency, the cells ($\sim 10 \times 10^6$) were transferred on ice, washed twice with ice-cold PBS, and pelleted by centrifugation at 300*g* for 5 min. Next, the cells were incubated with 1.0 ml of 0.5 M sodium bicarbonate buffer (pH 11) for 10 min and lysed with 1.0 ml of lysis buffer [1.0% (w/v) Triton X-100 in 25 mM tris-HCl (pH 7.4) and 100 mM NaCl] directly

onto the plate. After the plates were placed in a gyratory rocker for 20 min at room temperature, the lysate was transferred to a 2-ml all-glass homogenization tube, followed by 15 up and down strokes and sonication for 10 s. OptiPrep (Sigma-Aldrich) was diluted with the isolation buffer [150 mM NaCl, 5 mM dithiothreitol (DTT), 5 mM EDTA, and 25 mM tris-HCl (pH 7.4) with a protease inhibitor cocktail]. The density gradient at the bottom contained 35% and decreased to 30%, 25%, and 20%. After 167 μl of cell lysate was gently laid on the bottom and centrifuged at 160,000*g* in a TLA-55 rotor (Beckman, TL-100) for 4 hours at 4°C, the lipid raft fraction formed a white ring in the top layers and was collected with a sharp Pasteur pipette.

Antibody shift and immunoprecipitation experiments

Antibody shift experiments were performed using antibodies against StAR, GRP78, and COX-IV (Sigma-Aldrich), as identified by MS. Rat adrenals or testes were diced and resuspended in PBS, and the cellular debris was removed after centrifugation at 600*g* for 10 min. After the supernatant was transferred onto ice for 30 min, the cellular suspension or MA-10 cells were processed in a similar fashion. The cellular pellet was solubilized with 1% digitonin, and then specific antibody was added at a previously determined dilution for 60 min. The antibody complex was isolated by centrifugation at 9000 rpm (Beckman Allegra, F630 rotor) for 45 min, resolved by 4 to 16% native gradient PAGE, transferred to a polyvinylidene difluoride membrane, and stained with specific antibodies.

For immunoprecipitation, digitonin extracts were incubated overnight at 4°C with the indicated antibodies in 25 mM tris-HCl (pH 7.5), 1% Triton X-100, 0.5% NP-40, 200 mM NaCl, 0.5% sodium deoxycholate, and 1× protease inhibitor cocktail. The StAR preimmune serum was added as a negative control, and StAR antiserum was added as a positive control. Protein A–Sepharose CL-4B was used to isolate the protein-immunoglobulin complex. Adsorbed complexes were eluted by boiling for 15 min in 1× SDS sample buffer and analyzed by Western blotting.

Proteolytic digestion experiments

Proteolytic digestion experiments were performed at 4°C using various concentrations of PK (Sigma-Aldrich). The limited digestion experiments were performed using total cell lysate obtained after transfection of the WT or mutant StAR and different concentrations of PK for 30 min. The reactions were terminated by the addition of an equal volume of SDS sample buffer containing 2 mM PMSF and then by incubating in a boiling water bath. After electrophoresis, the samples were processed for Western blotting using the indicated antibodies.

[^{35}S]Methionine-labeled protein was synthesized following a CFS (cell-free system) using rabbit reticulocyte system following the manufacturer's procedure (Promega). Ribosomes and their associated polypeptide chains were removed by centrifugation at 150,000*g* for 15 min at 4°C, as previously described (*32*). For protease assays, the WT and mutant R182L StAR protein cell-free synthesized system reaction was incubated with a range of PK (0.1 to 0.5 μg/μl) for 30 min at 4°C. The reaction was stopped by addition of 2× SDS buffer followed by boiling in a water bath. The samples were analyzed by SDS-PAGE, fixed in methanol/acetic acid (40:10), dried, and exposed to a phosphorimager screen (digital autoradiography; Molecular Dynamics/GE Healthcare).

Cross-linking

In vitro cross-linking.

Isolated MAM fractions were incubated with various concentrations of BS3 or disuccinimidyl glutarate solubilized in dimethyl sulfoxide (DMSO). For DMSO solubilization of cross-linker, a stock concentration was made and then gradually diluted to a final working concentration of 1 or 10 mM that was prepared in the NaH_2PO_4 or Hepes buffer. The reactions were terminated either by transferring them on ice or by the addition of approximately 10 to 20 μl of 1.0 M tris buffer (pH 9.0) depending on the experimental requirement.

In vivo cross-linking.

To study direct interaction of proteins, in vivo cross-linking was performed, with a major modification of the procedure developed by Dettmer *et al.* (*33*). MA-10 cells (5×10^6) were grown in tissue culture dishes, washed twice with PBS at room temperature, and then collected by gentle scraping. Next, the cells were incubated with the cross-linker, BS3 or disuccinimidyl propionate, which was initially solubilized in DMSO to a working concentration of 50 mM. After the cells were incubated with 0.5, 1.0, 2.0, and 5 mM of the cross-linker at 37°C for 1 hour in a rotating shaker, the reaction was quenched by addition of 1 M tris (pH 7.6) to a final concentration of 50 mM for an additional 15 min at 4°C. To avoid any endogenous protease activity, a protease inhibitor cocktail (Pierce) was immediately added and incubated for an additional 15 min at room temperature. The cross-linked cells were collected by centrifugation at 3000 rpm and resuspended in 10 mM Hepes (pH 7.4). The organelle fractionation was performed following a standard procedure previously described (*29*, *34*).

Purification and identification of complexes from native PAGE and analysis of metabolic activity

Following native 3 to 16% PAGE, the region that may contain a StAR-associated complex was excised and reelectrophoresed vertically in a 4 to 16% native gradient gel under identical conditions overnight at 4°C. The gel was then stained with specific antibodies and exposed to an x-ray film. The corresponding exposed regions were excised and processed for MS analysis.

Density gradient ultracentrifugation

Complexes were resolved by a sucrose density gradient (top 10% to bottom 30%) with a cushion of 200 μl of 68% (2.0 M) sucrose to a final volume of 2 ml. Approximately 100 μl was layered on the top and centrifuged at 4°C in a Beckman TLA-55 rotor at 55,000 rpm for 4 hours. After centrifugation, fractions of 125 μl were collected. Gradient fractions were analyzed by native PAGE to show that the complexes were not degraded during the sucrose density gradient resolution and subjected to immunoprecipitation to determine StAR-specific interactions. An aliquot of 20 μl was used for both the immunoprecipitation and Western blotting.

Metabolic steroid conversion assays

Isolated mitochondria from mice adrenals or steroidogenic MA-10 cells (300 μg) were incubated in phosphate buffer (pH 7.4) to measure the metabolic conversion of [^{14}C]cholesterol to pregnenolone. We considered 80,000 counts of [^{14}C]cholesterol for each reaction and chased with 20 μg of unlabeled cholesterol. The metabolic conversion was initiated by addition of NADPH (reduced form of nicotinamide adenine dinucleotide phosphate), and the reaction mixture was similarly incubated at 37°C water bath with continuous shaking for 3 hours. To ensure complete conversion, we also used fivefold excess cold carrier to reach the saturation point. The newly synthesized steroids were extracted with ether/acetone (9:1, v/v), and an equal amount of cold cholesterol-pregnenolone mixture in CH_2Cl_2 was added as a carrier. The organic extracts were concentrated under a stream

of nitrogen or air and then separated by thin-layer chromatography (Whatman) using a chloroform/ethyl acetate (3:1) mobile phase. For accurate identification of steroids, the spots from the silica plates were extracted with organic solvents following our established procedure (*35*) and then analyzed by gas chromatography–MS (*36*).

EM to identify the kinetics of expression

EM was performed following our previously reported procedure with no modification (*37*). The anti-StAR, anti-GRP78, anti-Caln, and anti–aldosterone synthase antibodies were diluted 1:1000 in PBS containing 0.4% BSA. Anti-Tom22 was diluted 1:500 in the same solution. Semi-quantitative analysis was performed on all grids, with each image divided into 16 quadrants for counting the number of gold particles. To avoid any error, we counted each image five times, and SD was determined. Results were expressed as the number of gold particles per field of view. Field of view sizes were calculated using the quantitation function of the Gatan Microscopy Suite software (Gatan Inc.).

Mass spectrometry

Stained protein bands were excised, destained, reduced with DTT (Roche), alkylated with iodoacetamide (Sigma-Aldrich) and digested with trypsin (Promega) overnight, and processed for liquid chromatography–MS/MS on a nanoACQUITY HPLC system (Waters) coupled with a Q-Tof Premier mass spectrometer (Micromass/Waters) following an identical procedure as previously described (*16*, *29*).

Figure preparation

Data were obtained from the autoradiogram or from scanning through a phosphorimager. Some figures were generated by selecting specific lanes from the same autoradiogram or from two different autoradiograms, where the parallel experiments were performed at the same time.

SUPPLEMENTARY MATERIALS

Supplementary material for this article is available at http://advances.sciencemag.org/cgi/content/full/3/2/e1602038/DC1

Supplementary Results

fig. S1. EM analysis of testicular tissues with a StAR and GRP78 antibody.

fig. S2. Identification of compartment-specific localization of StAR and GRP78 in rat testes (right) and cAMP-stimulated MA-10 cells (left).

fig. S3. Kinetics of StAR folding by GRP78.

fig. S4. EM colocalization kinetics of aldosterone synthase (A), Tom22 (B), and Caln (C) in MA-10 cells in total and mito lane.

fig. S5. EM colocalization kinetics of StAR and GRP78 after cAMP stimulation after staining with StAR and GRP78 antibodies together.

fig. S6. Colocalization kinetics of StAR and GRP78 after cAMP stimulation.

fig. S7. Colocalization kinetics of WT (top) and mutant R182L (middle) StAR after cAMP stimulation.

table S1. One-dimensional native PAGE (3 to 16%) of mitochondrial-associated membrane native complex stained with StAR antibody (450-kDa MAM complex).

table S2. One-dimensional native PAGE (3 to 16%) of mitochondrial-associated membrane native complex stained with GRP78 antibody (450-kDa MAM complex).

table S3. Chemical cross-linked complex analysis (135-kDa complex).

REFERENCES AND NOTES

1. C. A. Mannella, K. Buttle, B. K. Rath, M. Marko, Electron microscopic tomography of rat-liver mitochondria and their interaction with the endoplasmic reticulum. *Biofactors* **8**, 225–228 (1998).
2. G. Csordás, C. Renken, P. Várnai, L. Walter, D. Weaver, K. F. Buttle, T. Balla, C. A. Mannella, G. Hajnóczky, Structural and functional features and significance of the physical linkage between ER and mitochondria. *J. Cell Biol.* **174**, 915–921 (2006).
3. B. Kornmann, E. Currie, S. R. Collins, M. Schuldiner, J. Nunnari, J. S. Weissman, P. Walter, An ER-mitochondria tethering complex revealed by a synthetic biology screen. *Science* **325**, 477–481 (2009).
4. J. E. Vance, Phospholipid synthesis in a membrane fraction associated with mitochondria. *J. Biol. Chem.* **265**, 7248–7256 (1990).
5. M. Lebiedzinska, G. Szabadkai, A. W. E. Jones, J. Duszynski, M. R. Wieckowski, Interactions between the endoplasmic reticulum, mitochondria, plasma membrane and other subcellular organelles. *Int. J. Biochem. Cell Biol.* **41**, 1805–1816 (2009).
6. C. M. Dobson, Protein folding and misfolding. *Nature* **426**, 884–890 (2003).
7. R. R. Kopito, Aggregosomes, inclusion bodies and protein aggregation. *Trends Cell Biol.* **10**, 524–530 (2000).
8. Z. Kostova, D. H. Wolf, For whom the bell tolls: Protein quality control of the endoplasmic reticulum and the ubiquitin-proteasome connection. *EMBO J.* **22**, 2309–2317 (2003).
9. B. Bukau, A. L. Horwich, The Hsp70 and Hsp60 chaperone machines. *Cell* **92**, 351–366 (1998).
10. F. U. Hartl, M. Hayer-Hartl, Molecular chaperones in the cytosol: From nascent chain to folded protein. *Science* **295**, 1852–1858 (2002).
11. Y. Ma, L. M. Hendershot, The role of the unfolded protein response in tumour development: Friend or foe? *Nat. Rev. Cancer* **4**, 966–977 (2004).
12. D. M. Stocco, B. J. Clark, Regulation of the acute production of steroids in steroidogenic cells. *Endocr. Rev.* **17**, 221–244 (1996).
13. H. S. Bose, T. Sugawara, J. F. Strauss III, W. L. Miller; International Congenital Lipoid Adrenal Hyperplasia Consortium, The pathophysiology and genetics of congenital lipoid adrenal hyperplasia. *N. Engl. J. Med.* **335**, 1870–1879 (1996).
14. M. Bose, R. M. Whittal, W. L. Miller, H. S. Bose, Steroidogenic activity of StAR requires contact with mitochondrial VDAC1 and phosphate carrier protein. *J. Biol. Chem.* **283**, 8837–8845 (2008).
15. H. S. Bose, Mechanistic sequence of mitochondrial cholesterol transport by StAR proteins. *J. Proteins Proteom.* **2**, 1–9 (2011).
16. M. Prasad, J. Kaur, K. J. Pawlak, M. Bose, R. M. Whittal, H. S. Bose, Mitochondria-associated endoplasmic reticulum membrane (MAM) regulates steroidogenic activity via steroidogenic acute regulatory protein (StAR)-voltage-dependent anion channel 2 (VDAC2) interaction. *J. Biol. Chem.* **290**, 2604–2616 (2015).
17. W. L. Miller, H. S. Bose, Early steps in steroidogenesis: Intracellular cholesterol trafficking. *J. Lipid Res.* **52**, 2111–2135 (2011).
18. B. J. Clark, J. Wells, S. R. King, D. M. Stocco, The purification, cloning and expression of a novel luteinizing hormone-induced mitochondrial protein in MA-10 mouse Leydig tumor cells. Characterization of the steroidogenic acute regulatory protein (StAR). *J. Biol. Chem.* **269**, 28314–28322 (1994).
19. W. L. Miller, R. J. Auchus, The molecular biology, biochemistry, and physiology of human steroidogenesis and its disorders. *Endocr. Rev.* **32**, 81–151 (2011).
20. V. R. Lingappa, J. R. Lingappa, R. Prasad, K. E. Ebner, G. Blobel, Coupled cell-free synthesis, segregation, and core glycosylation of a secretory protein. *Proc. Natl. Acad. Sci. U.S.A.* **75**, 2338–2342 (1978).
21. C. P. Ponting, L. Aravind, START: A lipid-binding domain in StAR, HD-ZIP and signalling proteins. *Trends Biochem. Sci.* **24**, 130–132 (1999).
22. E. London, How principles of domain formation in model membranes may explain ambiguities concerning lipid raft formation in cells. *Biochim. Biophys. Acta* **1746**, 203–220 (2005).
23. D. Marsh, Cholesterol-induced fluid membrane domains: A compendium of lipid-raft ternary phase diagrams. *Biochim. Biophys. Acta* **1788**, 2114–2123 (2009).
24. K. Christinsen, H. S. Bose, F. M. Harris, W. L. Miller, J. D. Bell, Binding of steroidogenic acute regulatory protein to synthetic membranes suggests an active molten globule. *J. Biol. Chem.* **276**, 17044–17051 (2001).
25. D. C. Yaworsky, B. Y. Baker, H. S. Bose, K. B. Best, L. B. Jensen, J. D. Bell, M. A. Baldwin, W. L. Miller, pH-dependent interactions of the carboxyl-terminal helix of steroidogenic acute regulatory protein with synthetic membranes. *J. Biol. Chem.* **280**, 2045–2054 (2005).
26. H. S. Bose, R. M. Whittal, M. A. Baldwin, W. L. Miller, The active form of the steroidogenic acute regulatory protein, StAR, appears to be a molten globule. *Proc. Natl. Acad. Sci. U.S.A.* **96**, 7250–7255 (1999).
27. K.-S. C. Marriott, M. Prasad, V. Thapliyal, H. S. Bose, σ-1 receptor at the mitochondrial-associated endoplasmic reticulum membrane is responsible for mitochondrial metabolic regulation. *J. Pharmacol. Exp. Ther.* **343**, 578–586 (2012).
28. H. S. Bose, V. R. Lingappa, W. L. Miller, Rapid regulation of steroidogenesis by mitochondrial protein import. *Nature* **417**, 87–91 (2002).
29. K. J. Pawlak, M. Prasad, J. L. Thomas, R. M. Whittal, H. S. Bose, Inner mitochondrial translocase Tim50 interacts with 3β-hydroxysteroid dehydrogenase type 2 to regulate adrenal and gonadal steroidogenesis. *J. Biol. Chem.* **286**, 39130–39140 (2011).
30. A. Luria, V. Vegelyte-Avery, B. Stith, N. M. Tsvetkova, W. F. Wolkers, J. H. Crowe, F. Tablin, R. Nuccitelli, Detergent-free domain isolated from *Xenopus* egg plasma membrane with properties similar to those of detergent-resistant membranes. *Biochemistry* **41**, 13189–13197 (2002).
31. J. L. Macdonald, L. J. Pike, A simplified method for the preparation of detergent-free lipid rafts. *J. Lipid Res.* **46**, 1061–1067 (2005).

32. M. P. Schwartz, A. Matouschek, The dimensions of the protein import channels in the outer and inner mitochondrial membrane. *Proc. Natl. Acad. Sci. U.S.A.* **96**, 13086–13090 (1999).
33. U. Dettmer, A. J. Newman, E. S. Luth, T. Bartels, D. Selkoe, In vivo cross-linking reveals principally oligomeric forms of α-synuclein and β-synuclein in neurons and non-neuronal cells. *J. Biol. Chem.* **288**, 6371–6385 (2013).
34. M. Bose, D. Debnath, Y. Chen, H. S. Bose, Folding, activity and import of steroidogenic acute regulatory protein into mitochondria changed by nicotine exposure. *J. Mol. Endocrinol.* **39**, 67–79 (2007).
35. K. J. Pawlak, M. Prasad, K. A. McKenzie, J. P. Wiebe, C. G. Gairola, R. M. Whittal, H. S. Bose, Decreased cytochrome *c* oxidase IV expression reduces steroidogenesis. *J. Pharmacol. Exp. Ther.* **338**, 598–604 (2011).
36. M. Prasad, J. L. Thomas, R. M. Whittal, H. S. Bose, Mitochondrial 3β-hydroxysteroid dehydrogenase enzyme activity requires a reversible pH-dependent conformational change at the intermembrane space *J. Biol. Chem.* **287**, 9534–9546 (2012).
37. M. Rajapaksha, J. Kaur, M. Prasad, K. J. Pawlak, B. Marshall, E. W. Perry, R. M. Whittal, H. S. Bose, An outer mitochondrial translocase, Tom22, is crucial for inner mitochondrial steroidogenic regulation in adrenal and gonadal tissues. *Mol. Cell. Biol.* **36**, 1032–1047 (2016).

Acknowledgments: We are thankful to all the members of the Hoskins Research laboratory for their collegial support. M.P. is also thankful to M. Bose (Dipa) for critically reading the manuscript. **Funding:** This work was supported previously by a grant from the NIH (HD057876) and Anderson Cancer Institute to H.S.B. **Author contributions:** H.S.B. conceptualized the idea, designed experiments, analyzed the data, and wrote the manuscript. M.P., W.E.B., E.E.P., B.M., and R.M.W. performed experiments. K.J.P. participated in the initial stage of this project. M.P. prepared biochemical figures; H.S.B. prepared EM figures, schematic presentations, and cartoons. **Competing interests:** The authors declare that they have no competing interests. **Data and materials availability:** All data needed to evaluate the conclusions in the paper are present in the paper and/or in the Supplementary Materials. Additional data related to this paper may be requested from the authors.

Submitted 26 August 2016
Accepted 25 January 2017
Published 24 February 2017
10.1126/sciadv.1602038

Citation: M. Prasad, K. J. Pawlak, W. E. Burak, E. E. Perry, B. Marshall, R. M. Whittal, H. S. Bose, Mitochondrial metabolic regulation by GRP78. *Sci. Adv.* **3**, e1602038 (2017).